[Article ID] 1003- 6326(2002)05- 0862- 07

Imitation design of temperature field in coloring hot dip galvanization process①

LE Qi-chi(乐启炽)[1], CUI Jian-zhong(崔建忠)[1], ZHANG Xue-bin(张学宾)[2]
(1. The Key Laboratory of Electromagnetic Processing of Materials, Ministry of Education, Northeastern University, Shenyang 110004, China;
2. Department of Materials Science and Technology, Luoyang University of Technology, Luoyang 471039, China)

[Abstract] Colors were generated by preferential oxidation of the metals in coloring hot dip galvanization process, and the evolution of temperature field during cooling after hot dip would be responsible for the coloration results directly. The influences of bath temperature and velocity of steel strip moving on temperature field of the strip were calculated in continuous coloring hot dip galvanization process by means of the ANSYS/Thermal module. The factors were considered including convection heat transfer, latent heat during cooling, and heat radiation in calculation. The effects of temperature field on coloration of sheet steel samples were investigated.

[Key words] coloring hot dip galvanization; temperature field; coloration
[CLC number] TG 174.443 [Document code] A

1 INTRODUCTION

Coloring hot dip galvanization is a new technique of producing colored galvanized steel sheet. It utilized the trace elements as additives of coloration bath, and its preferential oxidation in the coating during coloring hot dip galvanization process results in various colors on the steel components. The most important factor of affecting coloration is the temperature of the strip, which results in the changes of the thickness and the composition of the oxidation film, and finally influences the colors of components[1~9]. Therefore, it is important whether theoretically or practically to study the effect of processing parameters on temperature field in the process. In this paper, the temperature field is simulated and compared with that of the experiments.

2 EXPERIMENTAL

The pretreatment processing for coloring hot dip galvanization is basically the same as the traditional hot dip galvanization, which including caustic alkali degreasing, acid pickling and flux applying, as shown in Fig. 1. The sheet samples of 08Al steel sheet were cold-rolled with 1.2 mm thickness and 50 mm × 70 mm size, which were punched a hole at its top where a wire was tied for hot dip operation. After the pretreated samples were hot dipped in coloring bath for about 1 min, they were taken out quickly, and placed in the air vertically. Continuous color changes occurred on the samples during cooling, and the starting times of new color presentation were noted.

Fig. 2 is the diagrammatic sketch of zinc pot for the continuous coloring hot dip galvanization process. The steel strip is made of Q235-B cold-rolled strip with dimension of 80.0 mm × 0.6 mm. The preheated steel strip (θ_{init} = 130 ℃) entered into the zinc pot at a slope angle, whose velocities are v = 0.03, 0.05, 0.07 and 0.10 m/s respectively. An immersing roll and a let-off roll were set under the bath and the outlet of steel strip respectively, which insure the strip to exit the pot vertically, and to be separated from the zinc ash and the oxide for improving its surface quality.

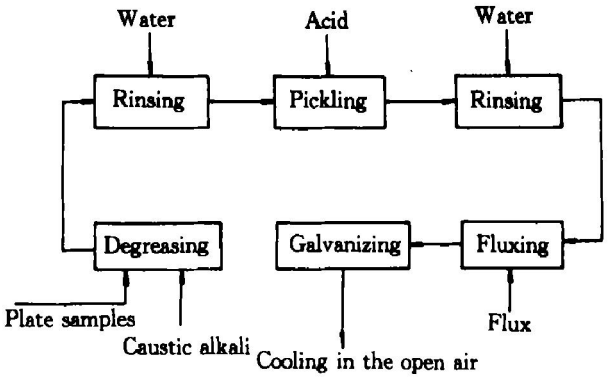

Fig. 1 Flowchart of coloring hot dip galvanization

3 BASIC HYPOTHESES FOR SIMULATION AND BOUNDARY CONDITION

3.1 Basic hypotheses

In order to simplify the calculation, the following hypotheses were made. The coloration bath was assumed as pure zinc bath ignoring the effect of additivesin the continuous galvanization process;

① [Received date] 2001- 10- 25; [Accepted date] 2001- 12- 28;

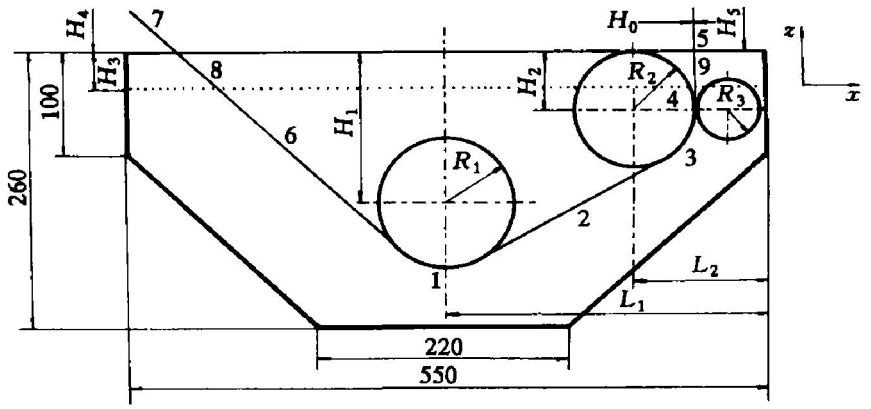

Fig. 2 Structure of zinc pot for continuous coloring hot dip galvanization
H_0= 0.6 mm, H_1= 145 mm, H_2= 60 mm, H_3= 40 mm, H_4= 100 mm, H_5= 300 mm, R_1= 55 mm, R_2= 50 mm, R_3= 27.5 mm, L_1= 275 mm, L_2= 110 mm

the material thermal properties of the strip was regarded as that of the plain carbon steel with 0.5% carbon; the pot was an isolator which insures bath temperature being constant; the fluid model for flowing via flat plate was used for the strip in the bath; the effects of the zinc coating and the flux on the heat transfer were ignored; and the physical properties of air were constant.

During calculating temperature field of static steel sheet block samples, convection heat transfer, heat emission, and the latent heat were included. The treatment of boundary conditions for convection was the same as that in the continuous coloring hot dip galvanization, ie, vertical flat plane mode.

Blackness, that is, emissivity, is defined as a ratio of radiometric force of the object and that of black body at the same temperature, which is related with material properties, temperature and its surface states (such as roughness, degree of oxidation).

Blackness of galvanized sheet is 0.28 at room temperature[10]. The blackness of metallic materials usually increases with increasing its temperature, and the roughness has certain effect on the blackness too. The higher the roughness is, the larger the blackness is. In this project, the blackness was chosen as 0.4 for its radiation temperature and roughness being higher than that of general galvanized sheet.

The latent heat was considered by means of revised specific heat, i e, the thermal properties of materials were regarded as functions of temperature. The equivalent specific heat capacity(c^*) and equivalent conductivity factor(λ^*) were defined as[11]:

$$c^*(\theta)=\begin{cases} c_1(\theta), & \theta< \theta_s, \\ \dfrac{c_1(\theta)+c_2(\theta)}{2}+\dfrac{Q}{\Delta\theta_s}, & \theta_s\leqslant\theta\leqslant\theta_l \\ c_2(\theta), & \theta> \theta_l \end{cases} \tag{1}$$

$$\lambda^*(\theta)=\begin{cases} \lambda_1(\theta), & \theta\leqslant\theta_s, \\ \lambda_1(\theta)+\dfrac{\lambda_2(\theta)-\lambda_1(\theta)}{\theta_l-\theta_s}(\theta-\theta_s), & \theta_s\leqslant\theta\leqslant\theta_l \\ \lambda_2(\theta), & \theta\geqslant\theta_l \end{cases} \tag{2}$$

where c_2, c_1 —before and after solidification specific heat capacity, respectively; θ_l, θ_s —beginning and ending temperature of solidification (θ_l= 421 ℃, θ_s= 417 ℃), respectively; $\Delta\theta_s$ —temperature region of solidification; Q — latent heat of solidification; λ_1, λ_2 —actual coefficient of heat conductivity in solid and liquid state, respectively. The correction was little for the coefficient of heat conductivity and significant for the specific heat capacity.

Fig. 3 shows the coordination system for the sheet samples and the outlet of strip (segment of 5 & 9 of Fig. 2) and its mesh partition. 1/8 and 1/4 of samples were chosen as subject investigated according to its symmetry (dashed area). The thickness of sheet sample composed of the steel basement and the coating. The coating thickness is between 10~ 80 μm within bath temperature, θ_b= 440 ~ 600 ℃ according to the measurement and decreases with increasing θ_b. The rest will be obtained through linear interpolation.

3.2 Boundary condition

The circumstance of heat transfer for steel strip is the air contained in the zinc pot and the ambient air outside the pot. The heat boundary condition refers mainly to convection. The physical properties of fluid would affect heat convection (i. e. coefficient of heat transfer) greatly, which include specific capacity of heat (c_p), density (ρ), coefficient of heat conductivity (λ) and viscosity (ν), and so on. The boundary condition treatments are exposed as followings.

1) Coloring hot dip bath

Nusselt number of liquid metal as following through the flat plate is defined as[11]:

$$Nu=0.53P_e^{1/2}=R_e\cdot P_r=\frac{v_{strip}l}{a} \tag{3}$$

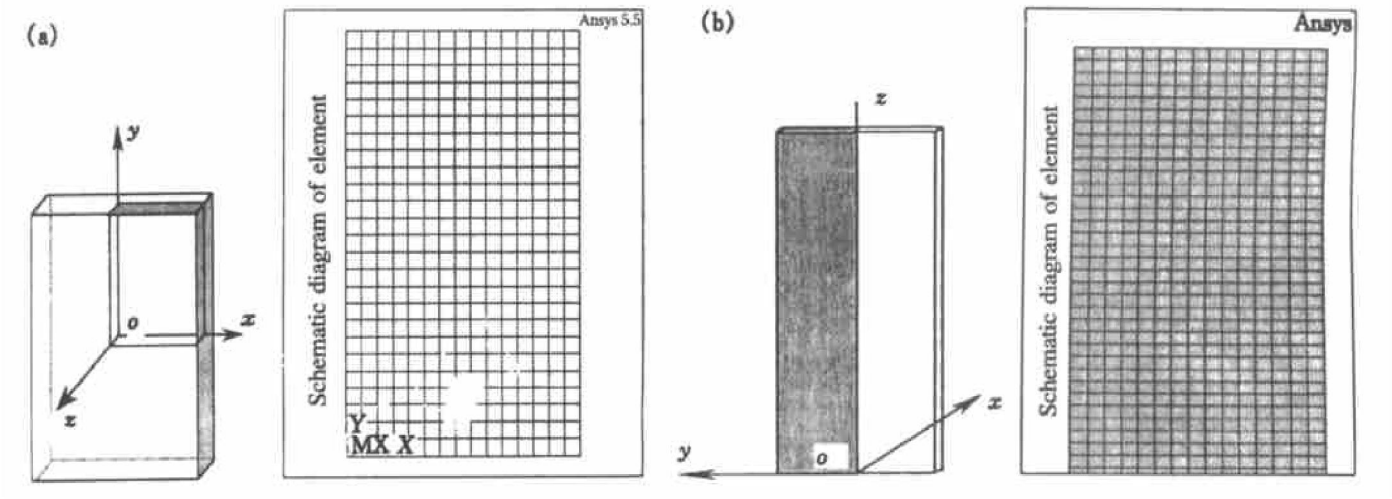

Fig. 3 Coordinate system and mesh partition
(a) —Sheet sample; (b) —Outlet of strip

where P_e —Peclet number, R_e —Reynolds number, P_r —Prandtl number, l —characteristic length (about 0.2 m), v_{strip} —Velocity of steel strip (m/s), a —Coefficient of temperature conductivity ($a = 7.83 \times 10^{-6} + 1.0 \times 10^{-8}\theta_b$ for zinc in this question).

2) Air

The empirical equation of natural-convection heat transfer in large space was applied to calculate the coefficient of heat transfer for convection between the strip and the air whatever inside or outside of the pot, the effect of kinematic velocity of the strip was ignored. The equation of natural-convection heat transfer in large space used widely in engineering can be determined from[11]:

$$Nu = C(G_r P_r)^n = C(\beta g \Delta t l^3 P_r / \mu^2)^n \quad (4)$$

where G_r —Grashof number, C —Constant, β —Dilatation coefficient of fluid ($\beta = 1/\theta$, 1/K), g —Gravitational acceleration(m/s^2), l —Typical dimension (outside pot: 0.3 m; inside pot: 0.04 m), $\Delta\theta$ —temperature difference between fluid and wall (℃), (10 ℃ for the ambient air and θ_b-50 ℃ for the air inside the pot), μ —kinematic coefficient of viscosity (1.416×10^{-5} m^2/s for air at 10 ℃).

Table 1 is the Prandtl number of air for the vertical flat plate within the test temperature (440~ 600 ℃).

Table 1 Prandtl number of air[11]

θ/ ℃	P_r
10	0.705
300	0.674
350	0.676
400	0.678
500	0.687
600	0.699

It is laminar flow due to the calculated $G_r P_r < 10^9$, the parameters in Eqn. 4 can be chosen as $C = 0.59$ and $n = 1/4$. Therefore, Nusselt number at the different temperature can also be obtained. Coefficient of convection heat transfer α is:

$$\alpha = Nu\lambda / l \quad (5)$$

where l —characteristic length (0.2 m in the bath, 0.04 m in the air inside the pot, and 0.3 m in the ambient air).

4 HEAT TRANSFER MODEL

The governing equations of fluid flow and heat transfer are a serials of differential equations composed of continuity equation, motion equation, and energy equation, which reflect the physical essences of mass, momentum, and energy conservation. The equations for incompressible fluid are[12]:

Continuity equation ($d\rho/dP = 1/\beta$ for the incompressible fluid, usually β selected as 10^5):

$$\frac{\partial \rho}{\partial t} + \sum_{i=x,y,z} \frac{\partial(\rho v_i)}{\partial i} = 0 \quad (6)$$

Motion equation (N-S equation):

$$\frac{\partial V_i}{\partial t} + \sum_{j=x,y,z} V_j \frac{\partial v_i}{\partial j} = F_i - \frac{1}{\rho}\frac{\partial p}{\partial i} + \nu \sum_{j=x,y,z} \frac{\partial^2 v_i}{\partial j^2} \quad (7)$$

Energy equation:

$$\rho C_p \frac{\partial \theta}{\partial t} + \rho C_p \sum_{i=x,y,z} \left[v_i \frac{\partial \theta}{\partial i} \right] = \lambda \sum_{j=x,y,z} \frac{\partial^2 T}{\partial j^2} + Q_v \quad (8)$$

where in Eqns. 6~ 8, v_l and F_i ($i = x, y, z$) are the components of velocity and mass in x, y, z directions respectively; ρ, ν, λ, C_p are density, kinematic viscosity, coefficient of heat conductivity, isobaric specific heat capacity; p, θ, t, Q_v are pressure, temperature, time, ratio of heat generation.

The 8-node hexahedron isoparametric element was chosen, and the Lagrange function is the interpolating function. Only the values of function at nodes are the unknown variables. The same interpolation function was used for the coordinating value and node function value. The temperature field is calculated after the velocity field is given out. The criterion of convergence is that the difference of temperature fields between the two adjacent time steps, ε, is less than the given small number, i. e.,

$$\varepsilon = \sum_{i=1}^{N}(\theta_i^k - \theta_i^{k-1}) / \sum_{i=1}^{N}\theta_i^k \leqslant \varepsilon_d \qquad (9)$$

where θ_i^k, θ_i^{k-1} are temperatures of k and $k-1$ step at node i, respectively; N is the total number of nodes. The judgment criterion of steady state is $\varepsilon_d = 1.0 \times 10^{-6}$.

5 RESULTS AND DISCUSSION

5.1 Temperature field of continuous coloring galvanization process

The calculating results indicated that the segment 6 of the strip reached steady uniform temperature field rapidly after entering into bath, so there is little effect on cooling rate of its outlet and would not influence the coloration of strip. Therefore, only segment 9 & 5 of the strip were analyzed mainly, wherein the velocity of strip and the bath temperature are the main variations.

Fig. 4 is the surface temperature fields of its outlet

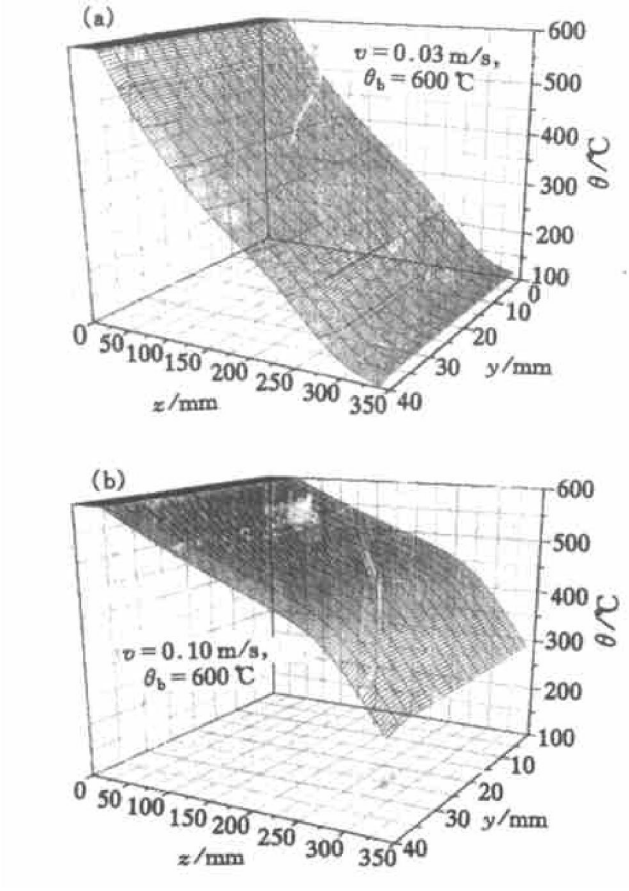

Fig. 4 Temperature field of outlet of strip at its different velocities

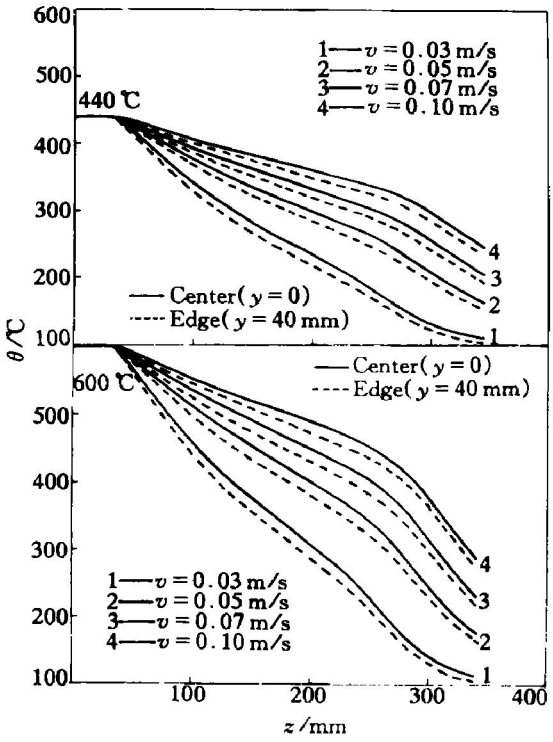

Fig. 5 Longitudinal temperature field for outlet of steel strip

$\theta(0.3, y, z)$ at $\theta_b = 600$ ℃, $v = 0.03$ and 0.10 m/s respectively. Fig. 5 is the steady longitudinal temperature distribution of the strip surface at 440 ℃ and 600 ℃, where the solid and dash lines represent the temperature of center ($y = 0$) and edge ($y = \pm 40$ mm) of the strip, respectively. It is obvious from Fig. 4 and Fig. 5 that the surface temperature of segment 9 of the strip kept uniform and no change basically, and that of segment 5 deceased rapidly. The strip velocity and the bath temperature were closely related with the degree of temperature drop. The lower velocity or the higher θ_b, the larger degree of temperature drops along the longitudinal direction, and the temperature of center is higher than that of edge along the transverse direction. The temperature difference of the strip is small along the transverse direction.

Fig. 6 is the temperature difference distribution of the strip along the lengthwise at 440 ℃ and 600 ℃. The transverse temperature differences along the lengthwise increase first and then drop down, which shows a peak that is gradually diminished with increasing v or enhanced and moved to the outlet direction of the strip with increasing θ_b. Fig. 7 is the relation of the maximal temperature difference with θ_b and v. It can be seen that the max increased linearly with increasing θ_b or decreasing v, except the velocity is lower than 0.05 m/s. Lowering θ_b or increasing v all are beneficial to decreasing the transverse temperature difference of the strip. However, if θ_b is too low the aimed colors will not achieved, and too high velocity of the strip will also bring on the difficulties in the actual operations.

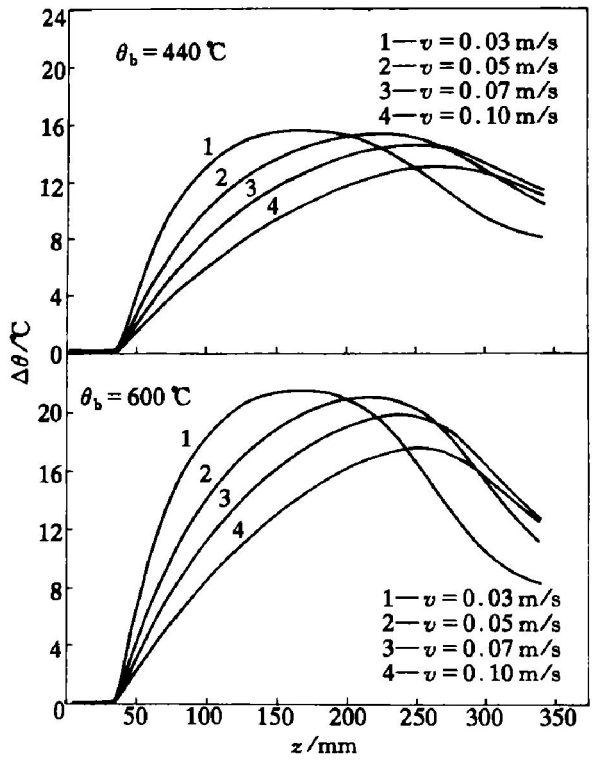

Fig. 6 Temperature difference along lateral direction for outlet of steel strip

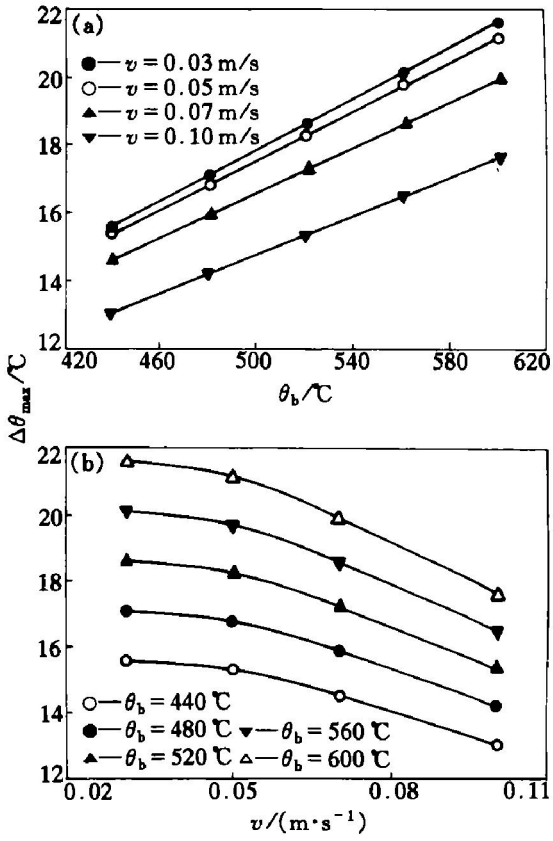

Fig. 7 Effect of θ_b and v on temperature difference along transverse direction for outlet of strip

Therefore, θ_b and v should be considered synthetically in order to obtain the desired coloration.

5.2 Effect of temperature field on coloration of sheet samples

Fig. 8 gives the isothermal lines of sample after cooled in air for 30 s at θ_b= 600 ℃. Fig. 8(a) indicates that the temperature difference in thickness is negligible. Therefore, it is enough to consider the temperature field of the surface layer only. From Fig. 8(b), the temperature drop at corners is faster than that of center, and the velocity gradient increases with increasing θ_b; the coating solidified completely after cooling for 30 s at θ_b= 600 ℃, which is consistent with the experimental fact that color changes can't exceed 30 s during cooling procedure.

Fig. 9 shows the variation of isothermal lines on the coating during cooled in ambient air after hot dipped in 440 ℃ and 600 ℃ bath, respectively. The solidification starting and ending point are 4.0 s and 4.9 s respectively for the former, and the latter is 26.1 s and 27.7 s, respectively. When the bath composition fluctuation occurred or the post-treatment carried out improperly, the color tone or the saturation degree of the samples may become non-

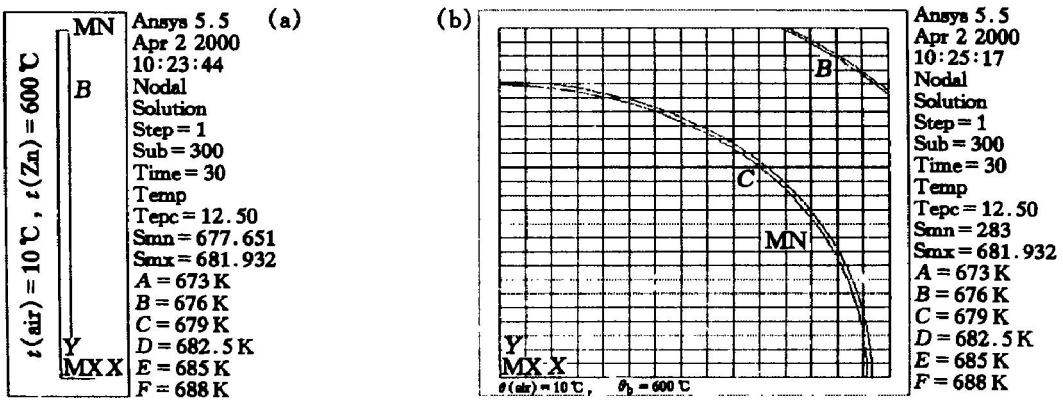

Fig. 8 Isothermal line at θ_b= 600 ℃ for sheet sample
(a) —Across thickness; (b) —Front view

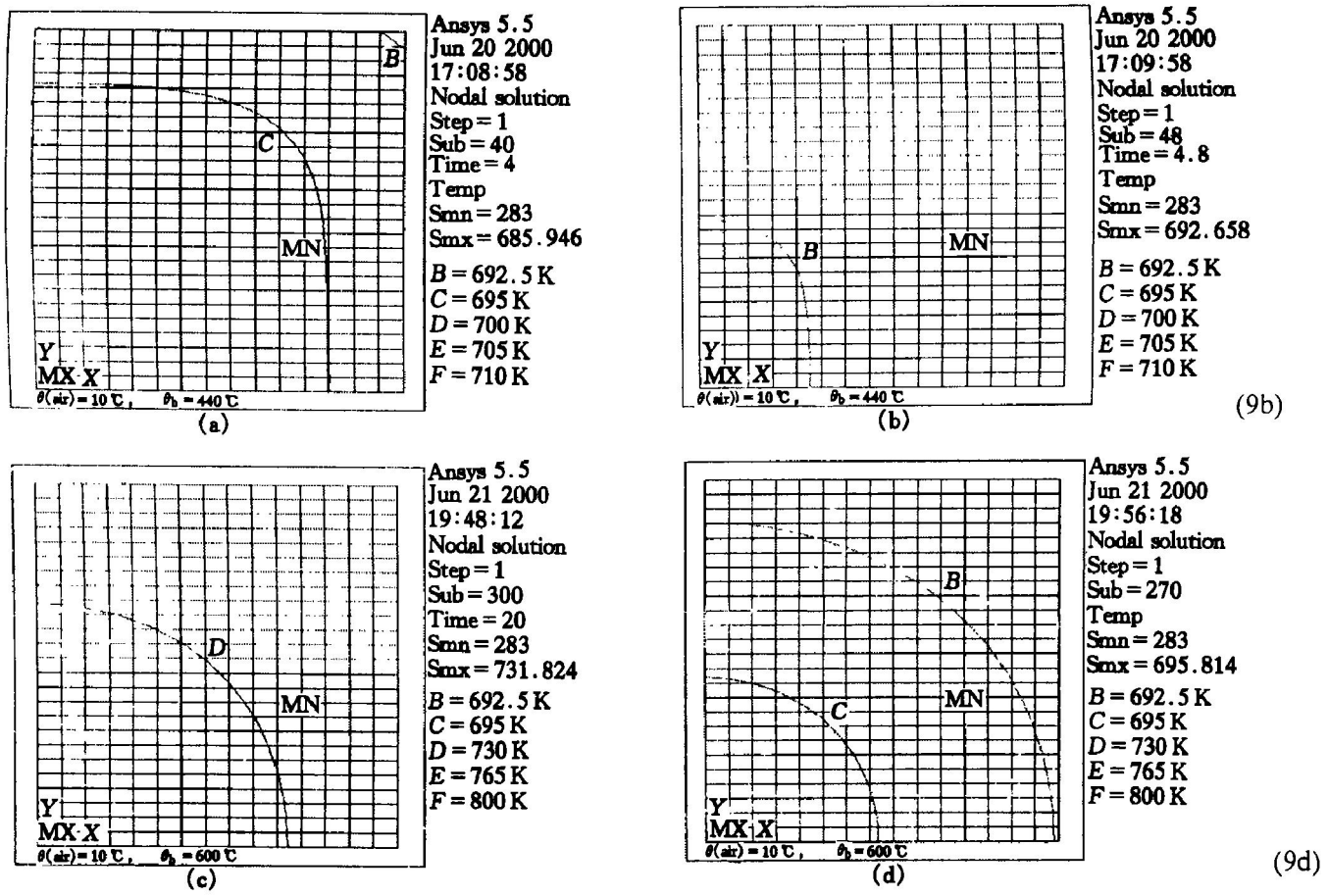

Fig. 9 Isothermal line as cooled in air after hot dipped at 440 ℃ and 600 ℃ for sheet sample
(a) —4.0 s; (b) —4.8 s; (c) —20.0 s; (d) —27.0 s

uniform at the non-homogeneous temperature. Fig. 10 gives the examples with non-uniform tone and saturation degree caused by larger temperature difference.

Because the color generation in this technology is owe to the preferential oxidation of the additive elements, and the oxidation is intimate relative with diffusion of additive elements, the velocity of which affects the kind of oxide and the construction of the oxide film directly, and of which is depend mainly on the state of coating. There is higher diffusion velocity before coating solidified, and it declines largely after solidification. Therefore, the solidification time is crucial to the color generation of coating. According to the calculation, the solidification starting and ending point (τ_b and τ_e) of coating were obtained for the samples cooled in ambient air (19~ 21 ℃) after lifting up from the different temperature bath (Fig. 11). It can be seen that solidification time is between 5 s and 27 s, τ_b and τ_e increase nearly linearly with increasing θ_b, the difference of which is not excess 2 s in a general way. In order to examine the calculation results, the τ_b and τ_e obtained from experiment were summarized for the samples after galvanized in the several binary alloy baths with different Mn contents. It should be pointed out that the color change is not significant any

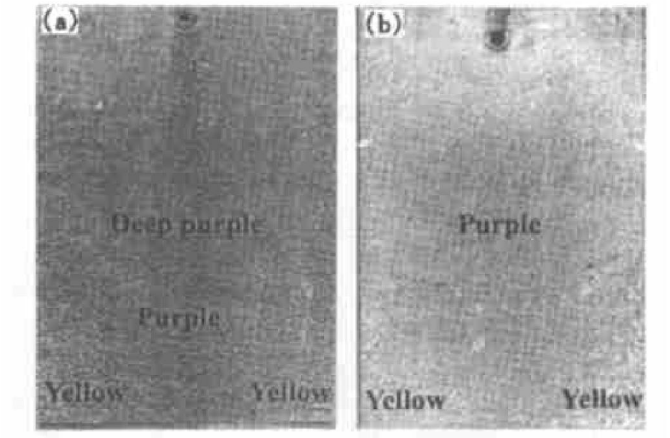

Fig. 10 Ununiformity of tone and saturation degree of color
(a) —Dipped in Zn-0.7Mn bath at 447 ℃ and cooled in air;
(b) —Dipped in Zn-0.3Ti-0.3Mn-0.1Ni-0.01Cu bath at 612 ℃ and cooled in 70 ℃ water

more on account of the diffusion of atoms decrease markedly after coating solidification, so it can be considered that the last color change time is correspondent to the solidification time. After comparing with τ_b and τ_e, although some of the experimental points are somewhat discrete, the calculation result is consis-

tent with that of the experimental on the whole. Another point should be noticed is that when the bath with few manganese (such as 0.2% and 0.4%) at higher θ_b, oxidation of manganese in coating reaches balance quickly due to the higher oxidation velocity, thereby, no significant color change occur after a very short time. In this case, the last color change point can not reflect the solidification time of coating.

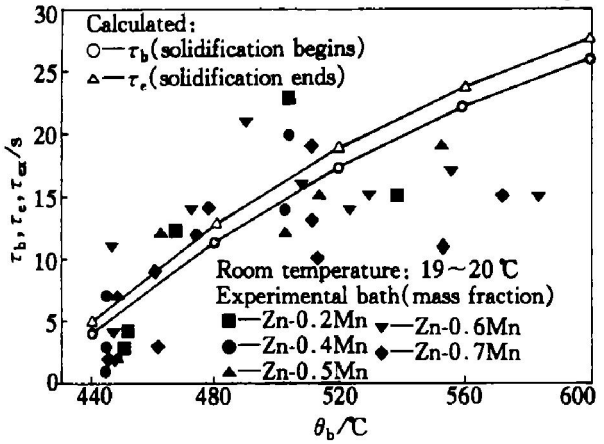

Fig. 11 Variation of τ_b and τ_e vs bath temperature

6 CONCLUSIONS

The strip reaches steady uniform temperature field rapidly after entering into bath, and that of outlet of the strip will affect the final coloration virtually; the temperature drops rapidly after exited from zinc pot, whose rate is closely related with θ_b and v. There is lower rate at lower θ_b or higher v, and the drop rate in the center is faster than the edge, which shows a peak in the center. The peaks lift up markedly with increasing θ_b and drop down gradually and move towards the outlet with increasing v. The max of transverse temperature increases linearly with increasing θ_b and decreases linearly with increasing v too, except the velocity of the strip is lower than 0.05 m/s.

After calculating the temperature field of static steel sheet samples during cooled in the air, the result indicates that the heat drop of corners is larger than that of center for samples, and the drop velocity gradient increases with increasing θ_b. When the bath composition fluctuation occurs or the post-treatment carried out improperly, the color tone or saturation degree of the samples may become non-uniform at the non-homogeneous temperature. The τ_b and τ_e increase nearly linearly with increasing θ_b, the difference of which is not excess 2 s in a general way. The results are consistent with that of the experimental on the whole.

[REFERENCES]

[1] Cominco Ltd. Process for the Production of Colored Coatings[P]. GB1195904, 1970.

[2] Robert W S, Gerald P L. Process for the production of colored coatings[P]. US3630792, 1971.

[3] Tomita M, Yamamoto S. Colored zinc coating[P]. EP0269005A2, 1987.

[4] Le Q C, Cui J Z. The influence of composition and temperature of bath and after-treatment on coloration in coloring hot dip galvanization[J]. Acta Metallurgica Sinica, 1999, 12(5): 1217-1222.

[5] LE Qi-chi, CUI Jian-zhong. The effect of Mn on coloring hot dip galvanization[J]. Materials Review, (in Chinese), 1999, 13(3): 63-65.

[6] LE Qi-chi, CUI Jian-zhong, HOU Chun-hong. Optimization of coloring galvanization baths[J]. The Chinese Journal of Nonferrous Metals, (in Chinese), 2000, 10(3): 388-394.

[7] LE Qi-chi, CUI Jian-zhong. Production and study on colored zinc coating steel sheet[J]. The Chinese Journal of Nonferrous Metals, (in Chinese), 1998, 8(Suppl. 2): 98-102.

[8] LE Qi-chi, LU Gui-min, CUI Jian-zhong. Activities of binary baths with 1% solute as standard states[J]. Trans Nonferrous Met Soc China, 2001, 11(3): 458-461.

[9] LU Gui-min, LE Qi-chi, CUI Jian-zhong. Thermodynamic properties of binary alloys of Zn-Mn & Zn-Ti[J]. The Chinese Journal of Nonferrous Metals, (in Chinese), 2001, 11(1): 95-98.

[10] CAI Qiao-fang. Heating Furnace, (in Chinese)[M]. Beijing: Metallurgical Industry Press, 1989: 268.

[11] ZHOU Jun-qing. Heat Transfer, (in Chinese)[M]. Beijing: Metallurgical Industry Press, 1992: 108, 139, 150, 162, 288, 289, 291.

[12] XU Wei-de. Fluid Mechanics (revised version), (in Chinese)[M]. Beijing: National Defence Industry Press, 1989: 44, 190.

(Edited by HUANG Jin-song)